valence state implying the role of electronic excitations in modifying the local electronic structures mainly the distortion in the TiO_6 octahedra. This study gives an insight about the role of structural properties and electronic structures in bandgap tuning [2].

REFERENCES:

[1] V. Kumar, A. Bhogra, M. Bala, S.C. Haw, C.L. Chen, C.L. Dong, K. Asokan, S. Annapoorni, Origin of intense blue-green emission in SrTiO3 thin films with implanted nitrogen ions: An investigation by synchrotron-based experimental techniques, Phys. Rev. B. **103**, 024104(2021). doi:10.1103/PhysRevB.103.024104.

[2] V. Kumar, A. Bhogra, M. Bala, H.-W. Kuo, C.-L. Chen, C.-L. Dong, A. Kandasami, A. Subramanian, Bandgap engineering in SrTiO3 thin films by electronic excitations: A synchrotron-based spectroscopic study, Scr. Mater. **195**, 113725(2021). doi:10.1016/j.scriptamat.2021.113725.

5.2.12 Pinning-assisted out-of-plane anisotropy in reverse stack FeCo/FePt intermetallic bilayers for controlled switching in spintronics

Garima Vashisht[1], Utkarsh Shashank[2], Surbhi Gupta[2], Rohit Medwal[3], C.L. Dong[4], C.L. Chen[5], K. Asokan[6], Y. Fukuma[2], S. Annapoorni[1,*]

[1]*Department of Physics and Astrophysics, University of Delhi, Delhi-110007, India*

[2]*Department of Physics and Information Technology, Faculty of Computer Science and System Engineering, Kyushu Institute of Technology, Iizuka, Fukuoka 820-8502, Japan*

[3]*Natural Sciences and Science Education, National Institute of Education, Nanyang Technological University, Singapore 637616*

[4]*Department of Physics, Tamkang University, Tamsui, 251 Taiwan*

[5]*National Synchrotron Radiation Research Center, Hsinchu, 30076, Taiwan*

[6]*Material Science Division, Inter University Accelerator Centre, Aruna Asaf Ali Marg, New Delhi-110067, India*

The magnetization reversal and anisotropy modulations in FeCo/FePt multilayers deposited on SiO_2/Si <100> substrates using RF magnetron sputtering was studied (refer Journal of Alloys and Compounds, 877 (2021) 160249 for details). The study presents an effective pathway to modify the anisotropy of FePt/FeCo multilayers via defect-mediated domain wall propagation. The effect of reversing the stack order of FeCo/FePt bilayers over oxidized Si substrate before and after providing thermal treatment at 500 ˚C is demonstrated. Rutherford Backscattering (RBS) spectrometry was performed at IUAC, New Delhi to estimate the film thickness and chemical composition of each layer along the depth of samples as a function of reversing the stacking order and post-annealing kinetics. He^{2+} ions with 2 MeV energy are incident on the samples and the yield of backscattered ions is recorded as a function of energy. A typical RBS spectra and the corresponding depth profile for as prepared FePt/FeCo/Substrate and FeCo/FePt/Substrate bilayers obtained by fitting the experimental RBS spectra using RUMP software is shown in figure 1. Both FePt and FeCo are present in the equi-atomic composition in all the samples. A slight surface oxidation of less than 1 nm is observed in all the bilayer series. The thickness of FeCo is 27 nm and 28 nm in the as-prepared samples FePt/FeCo/Si_As and FeCo/FePt/Si_As respectively. While for FePt, the thickness is 12.6 nm in both the series. After annealing the FePt/FeCo/Si series, a slightly diffused interface of 1 nm between FeCo and FePt layers is observed in FePt/FeCo/Si_500. On the other hand, the interface between two magnetic layers remains sharp for FeCo/FePt/Si_500. The structural, magnetic and electronic structure properties of FeCo/FePt exchange spring system prominently depend on the interfacial interactions between the two layers. The layered structure of FeCo/FePt/Si and FePt/FeCo/Si was probed at different depths using synchrotron X-ray diffraction to identify any probable strain developed at the interface. The in-plane M-H loops demonstrate a soft ferromagnetic behaviour in all bilayered samples, while the out-plane M-H loops shows two-step magnetization reversal with high coercivity. The rise in coercivity for out-plane configuration is attributed to the pinning dominated domain wall propagation. The out of plane magnetization of FePt is established in FeCo/FePt/SiO_2/Si series using ferromagnetic resonance and out-planeM-H curve measurements. In contrast to the high energy product generally attained in the FeCo/FePt multilayers, we demonstrate pinning-dominated coercivity mechanism in FeCo/FePt bilayers. Here the defects are created inevitably due to the interface of two layers without disturbing the crystallinity of the layers. After establishing the magnetic properties and magnetization reversal mechanism, the detailed investigation of electronic interactions between the atoms at the interface is studied by X-Ray Absorption spectroscopy and is subsequently related to the observed magnetic properties. The Fe, Co and Pt L-edge measurement indicates the electronic interactions between Fe-Co and Co-Pt after annealing FePt/FeCo/SiO_2/Si. While for FeCo/FePt/SiO_2/Si, the electronic interactions are prominent for Fe-Pt and Fe-Co. In conclusion, it was demonstrated that the stacking order of individual layers can be used as an ideal parameter to manipulate the anisotropy of FeCo/FePt system.

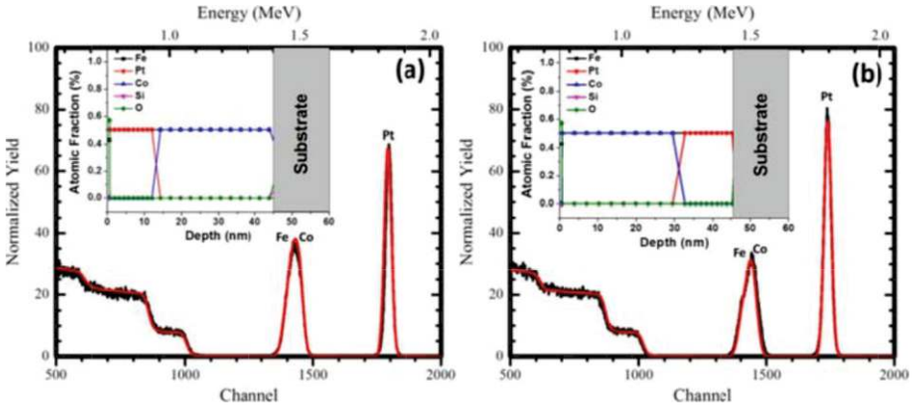

Figure 1. RBS spectra of (a) FePt/FeCo/Si and (b) FeCo/FePt/Si series.
The inset shows corresponding depth profile.

REFERENCES:

[1] G. Vashisht, U. Shashank, S. Gupta, R. Medwal, C. L. Dong, C. L. Chen, K. Asokan, Y. Fukuma and S. Annapoorni, Journal of Alloys and Compounds **877**, 160249(2021).

[2] L. Rebuffi, J. R. Plaisier, M. Abdellatief, A. Lausi and P. Scardi, Zeitschrift für anorganische und allgemeine Chemie **640**, 3100(2014).

5.2.13 Domain state modulation by interfacial diffusion in FePt/FeCo thin films: Experimental approach with micromagnetic modelling

Garima Vashisht[1], Zainab Hussain[2], Indra Sulania[3], Sunil Ojha[3], V.R. Reddy[2], S. Annapoorni[1]

[1]*Department of Physics and Astrophysics, University of Delhi, Delhi-110007*

[2]*UGC-DAE Consortium for Scientific Research, University Campus, Khandwa Road, Indore 452001, India*

[3]*Material Science Division, Inter University Accelerator Centre, Aruna Asaf Ali Marg, New Delhi-110067, India*

The magnetic properties of polycrystalline FePt/FeCo system, as a result of inter-diffusion between the two layers are demonstrated (refer Journal of Physics: Condensed Matter, 33 (2021) 335805). A comparative study is made for two systems viz. entirely diffused layers of FePt and FeCo giving rise to FeCo@FePt nano-composite like structures (sample S1); and layered FePt/FeCo system deposited with FeCo as an underlayer for FePt (sample S2). On post-annealing the FePt/FeCo/Si system, the phase conversion of FePt to $L1_0$ phase even at higher annealing temperatures could not be assured. Such consequences of post-annealing kinetics are examined by correlating the interfacial diffusion with structural variations in the two layers. The thickness and the depth profile as a result of thermal annealing were obtained by Rutherford Backscattering Spectroscopy (RBS) using a well-collimated beam of 2 MeV He^{2+} ions at IUAC, New Delhi. By fitting the RBS spectra using RUMP software, it is observed that sample S1 shows large diffusion of both the layers into each other giving rise to FeCo@FePt nano-composites like structures beneath 11 nm of FePt layer on top. The thickness of combined FeCo and FePt layers is ~ 125 nm. On the other hand, sample S2 shows a thickness of 11 nm FePt and 16 nm FeCo. The depth profile demonstrates a slight diffusion of FePt into the FeCo layer at the interface of 3 nm. This results in the formation of an interface with diffused FePt in the FeCo layer in sample S2. The electronic interactions between Co – Pt and Fe – Pt increase with enhanced diffusion between FeCo and FePt as observed from the X-ray absorption spectroscopy measurements performed at Fe and Co L-edge. The collective influence of such variations on the bulk and surface magnetic properties is investigated. The interfacial differences do not affect the bulk magnetic properties much in the in-plane configuration. However, remarkable differences are observed in the out-plane configuration. The out-plane hysteresis for entirely diffused magnetic layers exhibits a wasp-shape. In contrast, FePt/FeCo layers with a mild diffusion at the interface show random anisotropy in all three dimensions in the polycrystalline samples attributed to the interfacial imperfections. Magnetic force microscopy (MFM) images further provide evidence for the out-plane anisotropy in sample S2 i.e. FePt/FeCo layers with lesser diffusion. The magnetic domain structure of FeCo@FePt nano-composites (figure 1a) are consistent with the wasp – shaped out-plane hysteresis loop having low remanence. The maze – like pattern of magnetic domains (figure 1b) observed in FePt/FeCo/Substrate layers with lesser diffusion signifies the presence of perpendicular anisotropy in this system. The micromagnetic simulations predict that the experimentally obtained wasp-shaped hysteresis loop in the completely diffused layers is a manifestation of inhomogeneous anisotropies distributed along the plane of the film. These diffusion-mediated magnetic properties of the FePt/FeCo system are important to study for achieving the desired characteristics in the system.

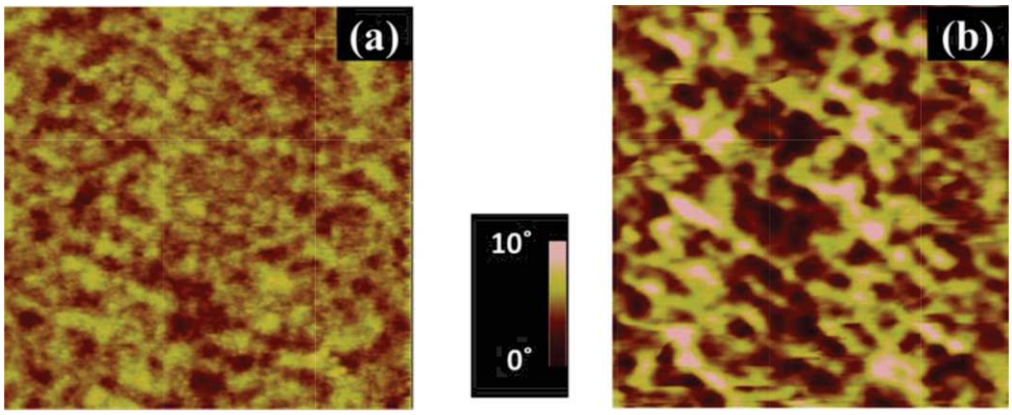

Figure 1. MFM image of sample (a) S1 and (b) S2.

REFERENCES:

[1] G. Vashisht, Z. Hussain, I. Sulania, S. Ojha, V. R. Reddy and S. Annapoorni, Journal of Physics: Condensed Matter **33**, 335805(2021).

5.2.14 Magnetization Reversal Behavior in Electrodeposited Fe–Co–Ni Thin Films

Kapil Dev [1], Rajdeep Kaur[1], Garima Vashisht[1], Indra Sulania[2], and S. Annapoorni

[1]*Department of Physics and Astrophysics, University of Delhi, New Delhi 110007, India*
[2]*Material Science Division, Inter University Accelerator Centre, New Delhi 110067, India*

The aim of the present work is to investigate the structural and magnetic behaviour of Fe-Co-Ni alloy thin films with increasing Ni concentration using electrochemical deposition. The effect of increasing Ni content on domain configuration and magnetization reversal behaviour is also investigated. Binary FeCo and ternary $(FeCo)_{(1-x)}Ni_x$ alloy thin films were deposited on ITO/glass substrate by electrochemical deposition. Pure FeCo film named as S1 and the FeCo films with 10, 16 and 25 at% of Ni were named as S2, S3 and S4 respectively. To investigate the effect of incorporation of Nickel on deposited nanostructures morphology and surface roughness, atomic force microscopy (AFM) measurements were performed in (AFM, Nanoscope IIIa) setup in lift height mode with the cantilever height at 40 nm. From the AFM images of sample S1 the uniform deposition of needle and rod like structures was confirmed, In S2, irregular rod like structures sandwiched between the granules are observed. A globular morphology was observed for sample S3 and S4. It is concluded that with increasing Ni content, the morphology evolves as granular structures. The rms surface roughness for FeCo films (S1) is 9.7 nm which reduced to 6.9 nm for sample S4 withincreasing Ni content. The gradual decrease in rms surface roughness with increasing Ni content is consistent with the literature.

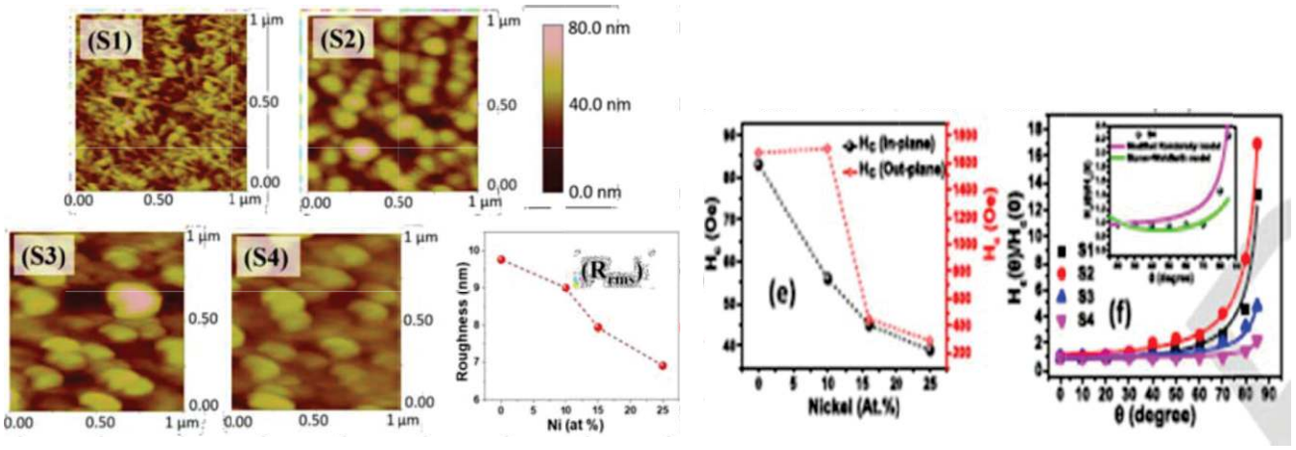

Figure 1: AFM image and magnetization behaviour for sample S1, S2, S3 and S4 with increasing Ni atomic %.

The hysteresis loops of Fe–Co–Ni films with 10%, 16%, and 25% Ni concentration were recorded and Fig. 1 summarizes the magnetic parameters as a function of varying Ni content. The in-plane Ms value of sample S1 (FeCo) is 1052 emu/cm^3, which decreases with the increasing concentration of Ni in the ternary Fe–Co–Ni alloy films. For samples S2, S3, and S4, the Ms values are 957, 819, and 655 emu/cm^3, respectively. The out-of-plane hysteresis does not saturate up to an applied field of 10 kOe. This is because of the easy axis oriented along the film plane, which makes it difficult to saturate the magnetic moments in the direction perpendicular to the film plane.

The experimentally observed magnetization reversal is explained by the presence of large pinning centers in FeCo, which reduced in size and density after the addition of Ni in FeCo alloy. Therefore, it is concluded that the morphology and magnetic properties in Fe–Co–Ni ternary alloy are strongly influenced by Ni content in the alloy. A thorough investigation of these properties as a function of controlled Ni content paves a way for the suitable designing of MEMS devices.

REFERENCES:

[1] R. Goyal, S. Lamba, and S. Annapoorni, "Growth of cobalt nanoparticles in Co-Al2O3 thin films deposited by RF sputtering," Phys. Status Solidi A, vol. **213**, no. 5, pp. 1309–1316, May (2016).

[2] Kapil Dev, Rajdeep Kaur, Garima Vashisht, Indra Sulania, and S. Annapoorni, Magnetization Reversal Behavior in Electrodeposited Fe–Co–Ni Thin Films, IEEE Transactions on Magnetics (In Press), March (2022).

5.2.15 Ion beam induced ionic conductivity of PVDF based separators for the energy storage device

Arshad A H[1], Santhosh Dani[1], S R Manohara[2], U V Khadke[1]

[1] *Department of Studies in Physics, Vijayanagara Sri Krishnadevaraya University, Ballari-583105, Karnataka, India.*

[2] *Department of Physics, SIT Tumukuru, Vishvesvarayya Technological University, Belgaum-06, India.*

We have synthesized pristine Polyvinylidene Fluoride (PVDF), PVDF-TiO2, PVDF-nTiO2, and PVDF-MWCNT composite thin films. Commercially available PVDF, MWCNT, and TiO2 were used in our research work. TiO_2 nanoparticles were synthesized by the combustion method using urea as fuel. PVDF, PVDF-MWCNT and PVDF-TiO_2 nanocomposite thin films of different stoichiometric ratios were prepared using the film casting technique [1]. The pristine PVDF thin film, TiO_2 nanoparticles, and PVDF nanocomposite thin films were characterized by XRD and FTIR spectroscopy. The XRD pattern of TiO_2 nanoparticles shows an anatase phase with a crystalline particle of size 55.98 nm estimated using Debye- Scherer equation. The XRD graph of pure PVDF shows the presence of b-phase. The FTIR spectra of prepared thin films in the wavenumber range 4000-400 cm^{-1} are obtained at room temperature. The FTIR spectra reveal the unequal and equal stretching vibrations of the CH_2 group in the PVDF matrix and the continuous band absorption region between 1450 and 1000 cm^{-1} corresponds to fluorocarbon absorption (C–F). The full set of characteristic vibrational bands (480, 510, 840, 882, 1071, 1401 cm^{-1}) indicates that the PVDF in the polymer matrix is retained in the β-phase.

Frequency-dependent dielectric properties of prepared pristine PVDF, PVDF-TiO_2 and PVDF-nTiO_2 thin films were studied using an LCR meter in the range of 50 Hz to 5 MHz. The dielectric constant of polymer nanocomposite thin films was found to decrease with the increase in frequency. The dielectric constant of PVDF- nTiO_2 increases with an increase in the wt% of filler compared to the PVDF-TiO_2.

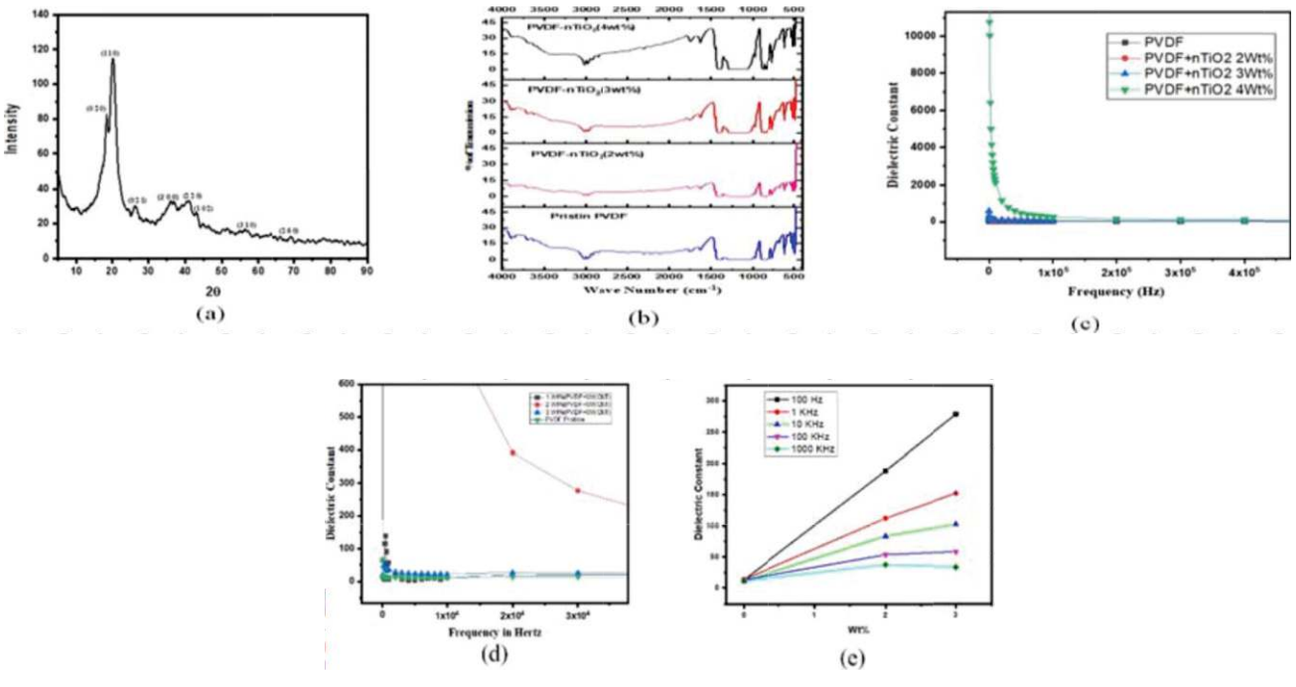

Fig.: (a) XRD of Pristine PVDF, (b)FTIR of PVDF& Nano composites, (c) Dielectric constant vs Frequency of PVDF+nTiO2 composites, (d) Dielectric constant vs Frequency of PVDF+MWCNT composites, (e) Dielectric constant vs wt% of PVDF+nTiO2 composites.

REFERENCES:

[1] Xia, Yang, *et al.* "Synthesis and electrochemical performance of poly (vinylidene fluoride)/SiO2 hybrid membrane for lithium- ion batteries." Journal of Solid-State Electrochemistry **23.2**, 519-527(2019).

[2] Monali V, *et al.* "Titanium dioxide/poly(vinylidene fluoride) hybrid polymer composite nanofibers as a potential separator for lithium battery". J. Mat. NanoSci. **4**(1), 6-12.

5.2.16 Noble Metal atoms implanted TiO_2 sensitized third generation solar cells

V. Bhullar[1], I. Singh[1], A. Mahajan[1*], F. Singh[2], D. D. Kshetri[2] and S. Chopra[2]

[1] *Department of Physics, Guru Nanak Dev University, Amritsar-143005, India*

[2] *Inter University Accelerator Center, New Delhi-110067, India*

Noble metal atoms doping in TiO_2 material (substitutional or interstitial) is of great interest as all the optical and electrical properties of TiO_2 material are site-selective [1-3]. It has been observed that ion implantation technique is a controlled way to incorporate noble metal atoms in TiO_2 nanomaterials. It has also been realized that, inclusion of one dimensional (1-D) TiO_2 nanofibers (NFs) increases light harvesting as well provides a fast charge transport network [4]. Another way to increase charge transport would be inclusion of $Ti_3C_2T_X$ based MXene in TiO_2 which would increase light scattering as well [5]. Thus TiO_2 NP-NF and TiO_2 NP-MXene based photoanode, implanted with noble metal atoms could be very crucial for all the photoelectrochemical applications especially TiO_2 sensitized mesoscopic solar cells. Keeping this in mind, thorough proposal has been planned with the objectives: 1) Implantation of noble metals (Au, Cu) for enhancing light harvesting and minimal recombinations in TiO_2 NP-NF and TiO_2 NP- MXene based photoelectrodes using low energy ion beam facility. 2) Fabrication and characterization of highly efficient and stable TiO_2 sensitized mesoscopic solar cells with prepared implanted photoanodes.

The proposed work was completed by firstly preparing TiO_2 NP-NF and TiO_2 MXene based photoelectrodes where TiO_2 NFs were prepared through electrospinning technique and MXene was prepared by etching Al from MAX. Photoanodes were prepared by initial deposition of a compact layer of TiO_2, prepared from titanium iso-propoxide solution, on pre-cleaned FTO substrates which were then kept for annealing at 450 ºC for 30 min. TiO_2 NFs (30 wt%)/MXene were mixed in TiO_2 NPs paste and the resulting mixture was doctor bladed with thickness 6 µm on compact layer deposited substrates and subsequently calcined for 30 min at 450 ºC. The prepared photoanodes were implanted with Au and Cu ions with 80 keV and 140 keV energy respectively at fluence of 1012 to 1015 ions.cm^{-2}.

Rutherford backscattering spectroscopy (RBS) was employed at IUAC on the implanted samples to confirm and quantify Au and Cu doping. The implanted photoanodes were further characterized for structural and optical properties using FESEM, XRD, XPS, UV-Vis, PL, and Raman and Kelvin probe spectroscopic techniques. From the XPS technique, the presence of substitutional and interstitial metal doping was confirmed. From the DFT simulations, it was observed that substitutional doping results in more impurity levels, lower band gap as compared to interstitial doping. Increase in the rutile content for substitutional over interstitial doping was realized from XRD measurements, which was responsible for effective light scattering. Moreover, from the UV-Vis absorption spectra it was observed that photo anodes with interstitial doping exhibit low light absorbance as compared to substitutionally doped photo anodes due to large band gap and distorted mesoporous TiO_2 structure on implantation. Work function measurements predicted upward shifting of the fermi level of TiO_2 on both substitutional and interstitial doping. Finally, the DSSCs and QDSCs prepared with substitutionally doped in TiO_2 was found to be more efficient than interstitially doped Au based DSSC owing to enhanced light harvesting, higher Fermi level and minimal recombinations as corroborated from UV-Vis, work function measurements and electrochemical impedance spectroscopy studies respectively.

REFERENCES:

[1] S. Khan, T. Lemes Ruwer, N. Khan, A. Köche, R. W. Lodge, H. Coelho-Júnior, R. L. Sommer, M. J. Leite Santos, C. F. Malfatti, C. P. Bergmann and J. A. Fernandes, Journal of Materials Chemistry A, **9**, 12214-12224(2021).

[2] S. K. Md Saad, A. Ali Umar, M. I. Ali Umar, M. Tomitori, M. Y. Abd. Rahman, M. Mat Salleh and M. Oyama, ACS Omega, **3**, 2579 2587(2018).

[3] L. Zeng, W. Song, M. Li, X. Jie, D. Zeng and C. Xie, Applied Catalysis A: General, **488**, 239-247(2014)

[4] V. Bhullar, S. Sardana and A. Mahajan, Solar Energy, **230**, 177-185(2021).

[5] Z. Shi, R. Khaledialidusti, M. Malaki, H. Zhang, Nanomaterials, **11**, 3170(2021).

5.2.17 Synthesis and diverse property studies on RGO based Ni-doped Cobalt oxide nanomaterials

Dake D. V.[1], Raskar N. D.[1], Mane V. A. [1], Sonpir R. B.[1] , K. Asokan[2], and B. N. Dole[1]

[1]*Department of Physics, Dr. Babasaheb Ambedkar Marathwada University, Aurangabad-431004, India.*

[2]*Materials Science, Inter-University Accelerator Centre, Aruna Asaf Ali Marg, New Delhi 110 067, India.*

All used chemicals were analytically pure grade, procured from Fisher Scientific Company, and without additional decontamination. Samples of RGO based Ni-doped Co_3O_4 nanocomposites were synthesized by the hydrothermal method. For the synthesis of RGO based Co_3O_4, 1M Cobalt acetate tetrahydrate (99%) and 1M Hexamine (99%), and 0.2 gm RGO were dissolved individually in distilled water. The Hexamine solution was added firstly in Cobalt acetate tetrahydrate solution under continuous stirring and after 20 min RGO was added to the above solution. Simultaneously with continuous stirring, ammonia was added drop-wise to maintain pH 12 and stirred the solution for 2h. The solution was transferred into the Teflon-lined stainless steel autoclave. Sealed the autoclave and kept it in a muffle furnace at 120 °C for 8 h. Cooled the system naturally at room temperature, the product was filtered and washed several times with distilled water, ethanol, and dried at room temperature. For the synthesis of RGO-based Ni-doped Co_3O_4 nanocomposites, Cobalt acetate tetrahydrate 0.95 M, Nickel chloride hexahydrate 0.05M (99 %), 1M Hexamine, and 0.2 g RGO were dissolved separately in 25 ml distilled water respectively. Mixed the above solution by adding ammonia to maintain pH 12and stirred the solution for 2h. The solution was transferred into the Teflon-lined stainless steel autoclave. Sealed the autoclave was kept in a muffle furnace at 120 °C for 8 h. The system was naturally cooled at room temperature, the product was filtered and washed several times with distilled water, ethanol and dried at room temperature.

X-ray diffraction (XRD) analysis is used to determine the crystalline structure of the synthesized porous Co_3O_4 NCs. Fig.1 depicts the XRD patterns of the synthesized porous Co_3O_4 nanoparticles which coincide with the diffraction peaks at 19.01° (111), 31.23° (220), 36.78°(311), 37.88° (222), 44.75° (400), 51.34° (331), 57.95° (422), 59.28° (511), 61.54° (220) and 65.17° (440). All observed diffraction peaks are in good agreement with the face-centered cubic structure of Co_3O_4 (JCPDS 42-1467), confirming the stoichiometric phase purity of pure cubic porous Co_3O_4 structure. Moreover, one other diffraction peak is located at 32.43^0 in Fig.1, suggesting that the synthesized

nanomaterials are Co_3O_4 without the presence of any other oxide forms. It is noticed that the intensity of one sample at (311) and intensity of three samples at (222) diffraction peak is much higher as compared to other peaks which indicates the preferential growth direction of (311) and (222) crystal planes respectively (Gwang-Su Jang et.al. Ceramic International). [*for details, see Ceramics International,* https://doi.org/10.1016/ *j.ceramint. 2017.09.217*].

The optical properties of the synthesized porous Co_3O_4 nanoparticles have been examined by measuring the UV- Vis and PL spectroscopies. Figure 2 shows the UV absorption spectrum of Co_3O_4 nanoparticles synthesized at constant calcination temperatures. Typically, the absorption peak at ~550 nm is associated with ligand–metal charge transfer of O^{2-}, Co^{2+} and $^{O2-}$, Co^{3+}, respectively. The optical band gaps of the system ~1.49 eV, 1.17eV, 1.25 eV, 0.89eV, and 0.81eV were estimated using the UV-Vis spectrum of porous pure Co_3O_4, Ni-doped Co_3O_4, RGO/ Co_3O_4 composite, RGO/ Ni-doped Co_3O_4 composite and RGO sample which corresponds to the samples have good conductivity. These observations suggest that the synthesized materials are Co_3O_4 with the obtained direct band energies. After calcination at 500 °C, the absorption peaks are slightly blue shifted and appear at a lower wavelength of ~550 nm which might be due to the change in nanoparticle morphology. The PL spectra of the synthesized Co_3O_4 nanoparticles are shown in Figure 3. The two emission peaks at ~525 nm in the visible region correspond to near band edge emission (NBE) which originated from the recombination of free excitons through an exciton–exciton collision process. A green and yellow emission at 564 nm and 590 nm is associated with deep-level emission (DLE) caused by the impurities and structural defects like oxygen vacancies and cobalt interstitials present in the Co_3O_4 crystal. The existence of strong UV emission and a suppressed green band confirms the good crystallinity of the as-synthesized porous Co_3O_4 nanostructured samples. (Hyung-Shik Shin et.al. Chem select) [2].

REFERENCES:

[1] Gwang-Su Jang, Sadia Ameen, M. Shaheer Akhtar, Hyung-Shik Shin, Ceramics International, https://doi.org/10.1016/ j.ceramint. 2017.09.217.

[2] Gwang-Su Jang, Sadia Ameen, Mohammad Shaheer Akhtar, Eunbi Kim, and Hyung- Shik Shin, ChemistrySelect **2**,8941 – 8949(2017). https://doi.org/10.1002/slct.201701571.

5.2.18 150 MeV Ag^{+11} swift heavy ion irradiation effects on spin coated BSFO/CFO/LNO for RRAM and magnetodielectric devices

Nisha Thankachen[1], A. Tripathi[2] and U.S. Joshi[1]

[1.] *Department of Physics, School of Sciences, Gujarat University, Ahmedabad – 380009, India.*

[2.] *Inter University Accelerator Centre, Aruna Asaf Ali Marg, New Delhi-110067, India*

Tailoring the multiferroic as wells as RRAM mechanism, we have synthesized $Bi_{0.6}Sr_{0.4}FeO_3$ /$CoFe_2O_4$/ $LaNiO_3$

(BSFO /CFO/ LNO) in a sandwiched layered structure on quartz substrate via sol gel spin coating method. This technique has been chosen for its simplicity in the fabrication process over others as it offers controlled growth of the thin film thickness, stoichiometry and smooth surface morphology at room temperature. LNO are good candidates for bottom electrode as perovskite oxides have been extensively studied for the fabrication of ferroelectric memory and micro sensor devices, conducting perovskite oxides are widely preferred as the bottom electrode [1]. Resistive switching (RS) phenomena induced due to electric field attract great attention because of its non-volatile applications. Furthermore, swift heavy ion (SHI) is a powerful tool to systematically create defects in a variety of systems to alter their electrical properties [2,3]. Three identical samples after all phase analysis were irradiated with 150 MeV Ag^{11+} ions at three different ion fluences. Study of RRAM mechanism and magnetodielectric measurements were conducted by using two probe method (Keithley 2450 SourceMeter) and GwInstek LCR - 8110G respectively. Ohmic electrical top electrode contacts of silver paste was coated on top of the deposited thin film for all electrical measurements of 500 µm diameter. Multiple voltage sweeps of -5 V to +5 V was employed to all the samples and simultaneously measuring the value of current in the presence and absence of magnetic field of 0.58 T. Dielectric and magnetodielectric measurements for the range of 20 Hz to 10 MHz was studied.

The effects and modifications caused because of swift heavy ion (SHI) irradiation on the electrical and magnetodielectric property of BSFO /CFO/ LNO thin films has been studied. Fabrication of LNO films is reported in ref. [1]. The films were quenched by drying the samples in a preheated furnace at 550 °C for 5 mins.

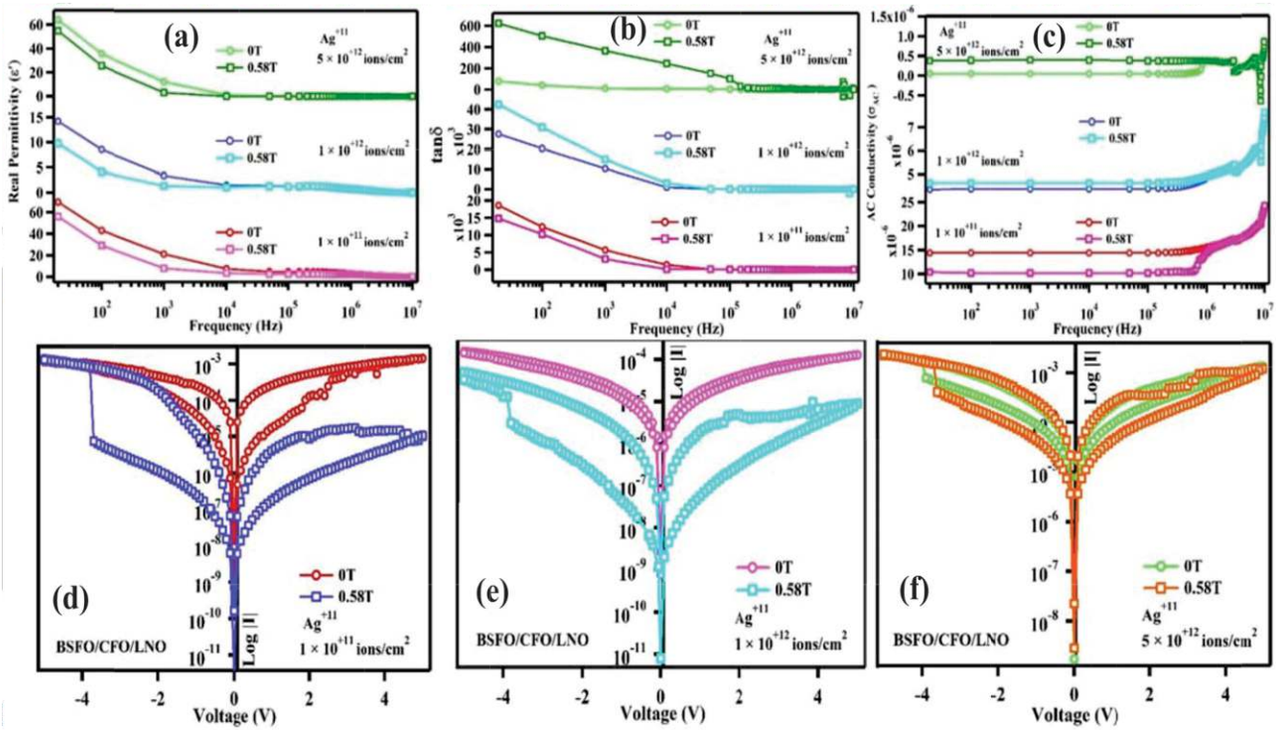

Figure 2. (a) Real permittivity, (b) Loss tangent (c) AC conductivity irradiated at $1 \times 10^{+11}$ ions/cm^2, $1 \times 10^{+12}$ ions/cm^2 and $5 \times 10^{+12}$ ions/cm^2 has been shown respectively. *I-V* characteristics has been shown in (d), (e) and (f) showing the change in RRAM behaviour with fluency.

Final annealing was done in an oxygen rich environment at 675 °C for 2 hours. Subsequently, the $Bi_{0.6}Sr_{0.4}FeO_3$ (BSFO) and $CoFe_2O_4$ (CFO) layers were deposited on conducting LNO bottom electrode by using solution processing. Surface and structural characterization was done by using AFM and XRD, respectively.

The multilayer films were irradiated using 15 UD Pelletron tandem accelerator at the Inter University Accelerator Centre (IUAC), New Delhi with 150 MeV Ag11+ ions at three different ion fluences i.e. $1 \times 10^{+11}$ ions/cm^2, $1 \times 10^{+12}$ ions/cm^2 and $5 \times 10^{+12}$ ions/cm^2 having a beam currents of 0.7 pnA. Figure 1 (a), (b) and (c) shows the magnetodielectric (MD) property for different irradiation fluences. At 1kHz, MD% for samples irradiated at $1 \times 10^{+11}$ ions/cm^2, $1 \times 10^{+12}$ ions/cm^2 and $5 \times 10^{+12}$ ions/cm^2 were found to be -62.55, -59.42 and -74.19, respectively. Defects created through Ag ions leads to an enhanced MD coupling. The point defects at the interface of the antiferromagnetic BSFO and ferromagnetic CFO seem to modify the magneto-transport of the devices. Figure 1. (d), (e) and (f) suggest an interesting hysteresis like behaviour in the *I-V* characteristics; a signature of resistive random access memory [4]. Further, the typical low resistance to high resistance ratios were found to enhance upon SHI irradiation. Further investigations of the role of ion and its different fluence are under process.